EXAMINATION OF THE SIZE AND MORPHOLOGY OF AUSTENITE GRAINS IN LAMELLAR GRAPHITE CAST IRON

Marcos G. López [ID]**, Juan M. Massone** [ID]**, and Roberto E. Boeri** [ID]
INTEMA, UNMdP - CONICET, Mar del Plata, Argentina

Abstract

There is a current discussion concerning the austenite grains of lamellar graphite irons and its growth at different carbon equivalent contents. The term "grain" is often employed to refer not only to the primary austenite, but also to the colonies or cells formed during the eutectic solidification. This investigation applies advanced experimental methods to study the solidification of lamellar graphite iron. A better understanding of the solidification process should lead to the design of better casting procedures. Samples of lamellar graphite iron were cast and directly austempered after solidification in order to reveal their solidification macrostructure. A typical ingot structure was found, with a narrow columnar-to-equiaxed transition. Electron backscatter diffraction technique was applied to confirm these macroscopic observations. Color etching was employed to determine the size of eutectic colonies at the columnar and equiaxed regions. The EBSD results confirm previous proposals, revealing that the solidification grains result from the growth of austenite dendrites. These grains include several eutectic colonies or cells inside, all these colonies or cells having the same crystalline orientation as the primary austenite dendrite. An analysis of the critical gradient for columnar-to-equiaxed transition could be developed. The size of the eutectic colonies at the columnar zone was found to be smaller than the size of the eutectic colonies at the equiaxed zone. Besides, the size of equiaxed grains strongly decreased with the increase in cooling rate, while no evident differences were obtained when the size of the columnar grains was measured.

Keywords: lamellar graphite iron, austenite grain, columnar-to-equiaxed transition, eutectic colony, EBSD, color etching

Introduction

Lamellar graphite cast iron (LGI) is a material that has been employed to satisfy engineering requirements for more than one century. Nowadays, it remains as one of the first choices as material for applications where the stiffness required for the component is more important than its tensile strength, such as internal combustion engine cylinder blocks, pump housings, valve bodies, and disk brake rotors. LGI stands out for its excellent thermal properties, high thermal conductivity and good specific heat capacity.

Despite being a relatively old material, there are still important aspects of LGI solidification that are not completely understood. The first works of Morrogh and Oldfield[1] employed drawings to account for the existence of large austenite dendrites that interacted with lamellar graphite cells in complex three-dimensional networks that defined the solidification structure. One of these drawings is shown in Figure 1.

Subsequently, Oldfield[2] carried out interrupted solidification experiments and obtained partially solidified samples that apparently showed the existence of independent solidification units conformed by austenite and graphite, denoted by some authors since thereafter as "eutectic grains." As the austenite dendrite arms were not directly observed in the plane of polishing of the sample, a speculation about the existence of a non-dendritic austenite

Figure 1. *Drawing of eutectic cell graphite with inter-penetrating austenite dendrites by Morrogh and Oldfield.*[1]

became popular.[3–5] From that moment on, several authors considered the existence of two different types of austenite, i.e., a dendritic austenite which is the result of primary solidification from the liquid, and a non-dendritic austenite produced during the cooperative growth with graphite at the eutectic reaction.

In the 1980s,[6] the advent of color etching techniques made it possible to reveal the first and last to freeze regions in the microstructure of cast iron samples. Through the use of these etching techniques, it was then possible to clearly identify the eutectic units first observed by Oldfield as well as the primary and secondary axes of the austenite dendrites.[7] However, the results of color etching micrographies could not clarify whether austenite dendrites and the eutectic units were part of a same solidification unit or whether they were produced by independent nucleation and growth processes.

In the 2000s, the technique of direct austempering after solidification (DAAS) allowed to obtain key information about the solidification of free graphite cast irons.[8,9] Relatively large austenite grains, sometimes with a narrow columnar-to-equiaxed transition, were now clearly visible by the naked eye. This was found to be true regardless of the carbon equivalent value.[10] Although the shape of these grains was evidently dendritic, some authors still were reluctant to accept that all the austenite present in an LGI sample was of dendritic nature and supported the existence of non-dendritic austenite at the eutectic units, mainly for eutectic and hypereutectic LGI.[11–13] Perhaps this was driven by the consideration of the classic literature prior to the 2000s,[4,5] when the DAAS method was still not developed.

Recently Stefanescu et al.[14] have proposed an updated explanation of the solidification process of LGI accounting for the latest experimental findings. Nevertheless, they still proposed that the formation of eutectic cells is the result of the independent nucleation and growth of austenite and graphite from the liquid for eutectic and hypereutectic LGI. They affirmed that these grains would be found inside the larger austenite grains observed by the naked eye by DAAS. This explanation was also included in a recent edition of the ASM Handbook dedicated to cast irons.[15]

Nevertheless, in a recent publication by the authors,[16] the proposal from Stefanescu et al. was refuted by applying EBSD to analyze the crystallographic orientation of the eutectic units and that of the primary austenite grains surrounding them. It was found that, even for eutectic and hypereutectic samples of LGI, the austenite present at the eutectic units was dendritic and that it had the same crystalline orientation as the primary austenite grains. This finding disregards the existence of "eutectic grains" of non-dendritic origin for LGI samples, regardless of their carbon equivalent. The terms "colony" or "cell" are then proposed to be used to refer to the units produced during the cooperative growth of austenite and graphite at the eutectic, as they are more appropriate than the term "grain."

Given the controversial explanations involving the cast iron solidification, the authors believe that it is a matter of crucial importance to clearly state how solidification of LGI proceeds based on the proper experimental evidence. This work attempts to clarify the solidification mechanism of LGI and to move forward on its study, gathering the findings from the last years regarding LGI solidification and extending to an analysis of the differences between solidification in columnar and equiaxed regions.

Methodology

Samples of LGI were cast in resin-bonded sand molds at the foundry laboratory of INTEMA. The chemical composition of the heat is listed in Table 1. Alloying with Cu and Ni is necessary to perform the DAAS procedure.[8] Melt was inoculated with 0.5% FeSi(75%Si) during tapping.

The samples obtained were treated according to the DAAS procedure to preserve their solidification macrostructure at room temperature. The procedure involved in DAAS has been extensively explained in the literature.[8]

The design employed for the casting was previously used to analyze the correlation between macrostructure and

Table 1. Chemical Composition of the Heat Produced

CE	C	Si	Cu	Ni	Mn	S	P
3.91	3.04	2.62	0.87	1.24	< 0.2	< 0.05	< 0.05

Values are Expressed in wt%

shrinkage porosity in spheroidal and compacted graphite iron.[17,18] This design has the particularity of presenting a variety of cooling rates which makes it suitable to study the columnar-to-equiaxed transition phenomena. It consists of three distinct volumes that can be handled separately after cutting. Figure 2 presents a schematic of the design indicating the three volumes denominated as V1, V2, and V3.

After sectioning, grinding, polishing, and etching with Nital 2%, it was possible to reveal the solidification macrostructure for each volume.

Subsequently, one sample was prepared to perform EBSD analysis at the Central Analytical Facility of the University of Alabama employing a Tescan Lyra FESEM equipped with an EDAX EBSD detector. The scan covered an area of 670 by 500 μm at steps of 0.5 μm. The indexed phases for the analysis were austenite and ferrite, leaving the graphite as non-indexed points. However, only the austenite phase was plotted in the inverse pole figures produced. No data cleaning routines were employed. High-angle grains boundaries were identified by misorientations of $\geq 10°$ between adjacent, indexed austenite points.

The samples were then subjected to a color etching to reveal the silicon depleted areas, which are known to be coincident with the last to freeze regions of the volumes. The area recorded for this analysis was several millimeters per side and located in such a way as to include the columnar-to-equiaxed transition region. In each columnar and equiaxial region the number of eutectic colonies and austenite grains per mm^2 was determined by the interception method described in ASTM E112-12.
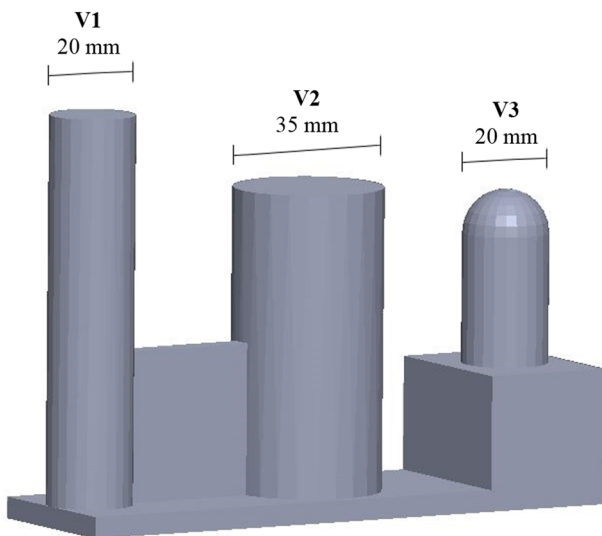
Finally, the software MagmaSoft® was employed to carry out numerical simulations of the filling and solidification of the experimental casting. The cooling rate and temperature gradient were calculated along the regions of the volumes analyzed microscopically. MagmaSoft® performs the calculations of these two criterions point to point at 2 °C above liquidus temperature.[19]

Results and Discussion

Study of the Solidification Macro and Micro Structure

The solidification macrostructures for the volumes V1, V2, and V3 are shown in Figure 3. The areas marked on the macrostructures correspond to the regions that were subsequently analyzed microscopically after color etching. The volumes in Figure 3 present relatively large austenite grains with a narrow columnar-to-equiaxed transition, such as it was formerly stated in the literature.[10,18] As expected, faster cooling rate regions show smaller grain size, while a much larger grain size is found at lower cooling rate portions.

In order to confirm the macroscopic observations from Figure 3, EBSD was applied at the equiaxed zone of the volume V1. The EBSD map obtained is shown in Figure 4. The crystallographic orientation is revealed as an inverse pole figure map with respect to the Z direction, normal to the surface of the sample. The EBSD map in Figure 4 shows the boundary between two equiaxed austenite grains, one presented in red and the other in blue according to their different crystallographic orientations. Small protrusions from at least two other neighboring grains are also

Figure 2. Schematic of the design employed for the castings indicating the three volumes, marked as V1, V2, and V3.
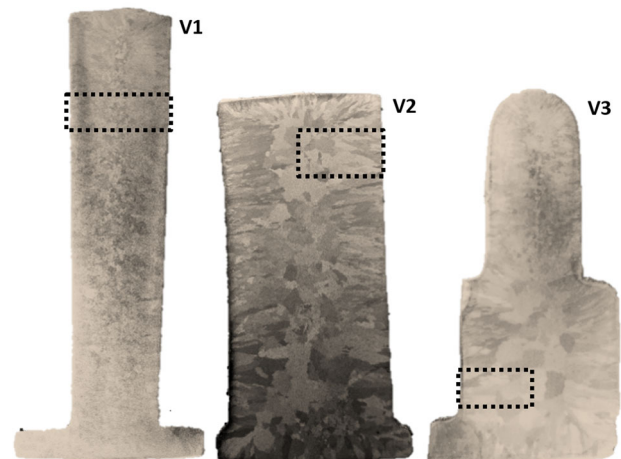
Figure 3. Solidification macrostructures obtained for volumes V1, V2, and V3. The marked regions show the zones where columnar-to-equiaxed transition was evaluated in Figures 8, 9 and 10.
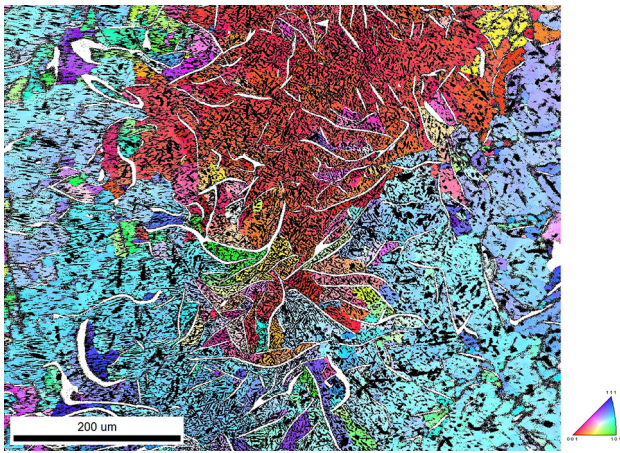
Figure 4. EBSD orientation map from the equiaxed region of volume V1.
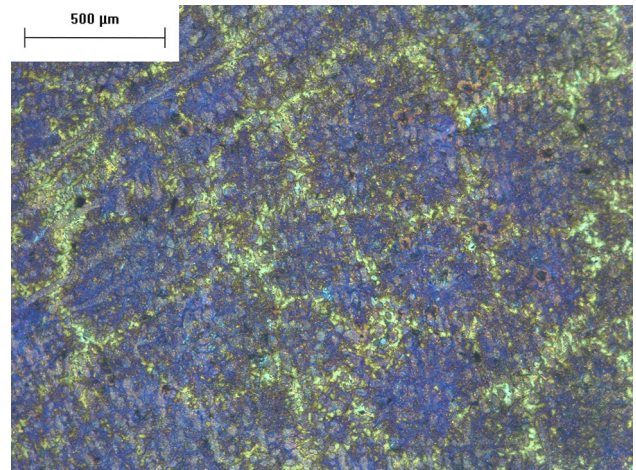

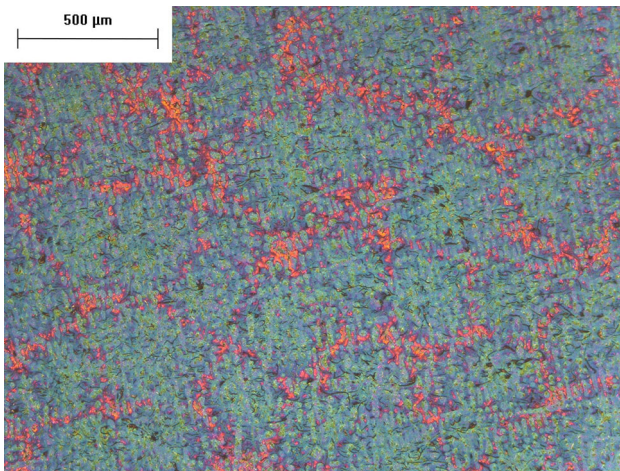*Figure 6. Color-etched microstructure obtained for volume V2.*

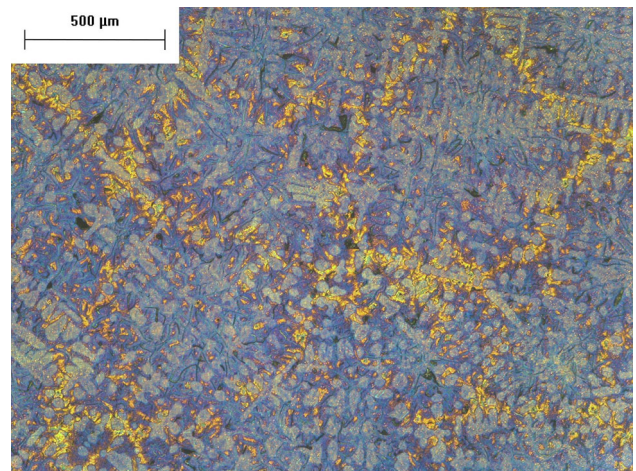*Figure 5. Color-etched microstructure obtained for volume V1.*

Figure 7. Color-etched microstructure obtained for volume V3.

observed. According to this observation and the results of previous studies,[16] it is possible to determine that all the eutectic colonies or cells have the same crystallographic orientation as their respective parent austenite grain. This means that the austenite dendrites conform the austenite that grows in contact with graphite at the eutectic colonies or cells.

Figures 5, 6, and 7 show the color-etched microstructures observed for the different volumes at the columnar zone as revealed after DAAS treatment shown in Figure 3. After color etching, the eutectic colonies or cells become visible and appear surrounded by the much brighter last to freeze zones. Color etching also reveals the presence of an extended network of primary and secondary austenite dendrite axes. The orientation of the primary axes matches the direction of growth of the columnar grains in Figure 3. In Figures 5, 6, and 7, a single austenite dendrite network extends through several colonies. So, these additional observations confirm that the colonies or cells are not

independent grains of austenite, since the austenite building them is the primary dendritic austenite, which covers several cells. Therefore, the term "eutectic grain" should not be used to refer to the units of cooperative growth between lamellar graphite and austenite dendrites; the terms "colony" or "cell" are considered as more suited to describe them. A more detailed study of this issue has already been published.[16]

Study of the Columnar-to-Equiaxed Transition

The color-etched surfaces of the selected areas of volumes V1, V2, and V3 were fully recorded by several micrographies. These were then stitched together in order to obtain a single image of the microstructure for the regions of interest marked in Figure 3. The position of the columnar-to-equiaxed transition was determined from the macrostructures shown in Figure 3, after a careful analysis of the columnar and equiaxed grains present in the selected regions of the figure. As the color-etched microstructures

from the regions marked in Figure 3 were also recorded, then it was possible to draw the columnar-to-equiaxed transition line directly upon the color-etched microstructure. The results are shown in Figures 8, 9, and 10.

Figures 8, 9, and 10 show that there is no sharp change in the cell structure or size as a result of the columnar-to-equiaxed transition. In order to further analyze the conditions that produced the transition observed between columnar and equiaxed grains the temperature gradient was calculated using MagmaSoft® at the columnar and equiaxed zones, as well as in the transition lines. The results are listed in Table 2.

Table 2 shows that the highest values of gradient are found for the columnar zone, while the lowest values are at the equiaxed region, as expected. Besides, a key feature to account is that a similar gradient of 1.1–1.2 °C/mm is found at the transition position for the three volumes studied. Consequently, there is a critical gradient at which columnar grains, that started growing with a higher gradient closer to the mold wall, stop their growth, giving place to the nucleation and growth of equiaxed grains in the remaining liquid with lower gradient. Although this gradient value is the result of a software calculation and not an experimental reading, it gives a first approximation to describe the columnar-to-equiaxed transition in LGI.

Influence of Columnar and Equiaxed Regions in the Distribution of Eutectic Colonies and Austenite Grains

Table 3 presents the number of colonies per mm^2 as measured from Figures 8, 9, and 10. It is observed that there is always a higher number of eutectic colonies per mm^2 in the columnar zone than in the equiaxed region. This means that the size of the eutectic colonies at the columnar zone is smaller than the size at the equiaxed regions.
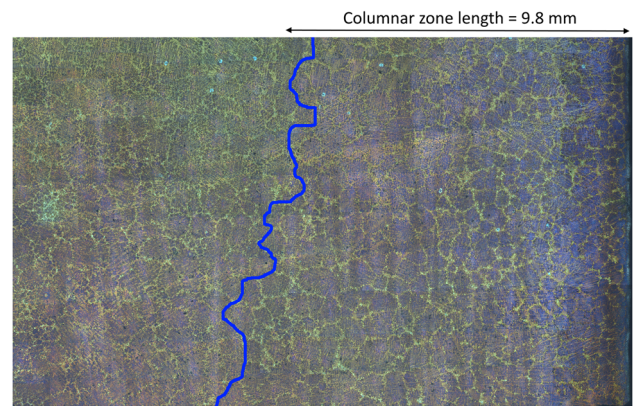

Figure 9. Color-etched microstructure of V2 on the region marked in Figure 3. Blue line marks columnar-to-equiaxed transition.

The cooling rate determined by MagmaSoft® is also listed in Table 4. As expected, for each volume, the cooling rate is always higher at the columnar than at the equiaxed zones.

Figure 11 shows a plot of the number of colonies per mm^2 in columnar and equiaxed regions as a function of cooling rate.

Table 5 shows the number of austenite grains per mm^2 for volumes V1, V2, and V3. It is found that there are also a higher number of grains per mm^2 in the columnar zone than in the equiaxed region, but only for the two volumes with the lowest cooling rate (V2 and V3). For the case of V1, which is the volume with the highest cooling rate according to Table 4, the austenite grains are smaller at the equiaxed zone than at the columnar region. This is observed as an inversion in the columnar/equiaxed ratio for the case of V1 in Table 5.

Figure 12 shows that the number of equiaxed and columnar grains per mm^2 are influenced by cooling rate. With the
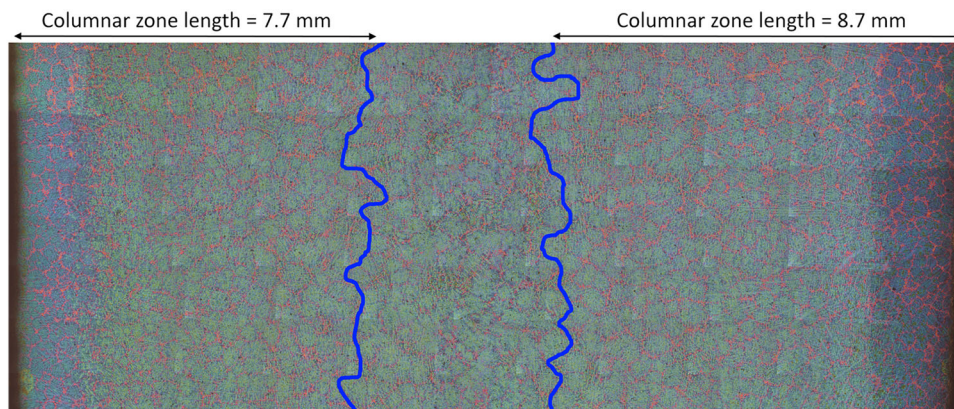

Figure 8. Color-etched microstructure of V1 on the region marked in Figure 3. Blue lines mark columnar-to-equiaxed transition.
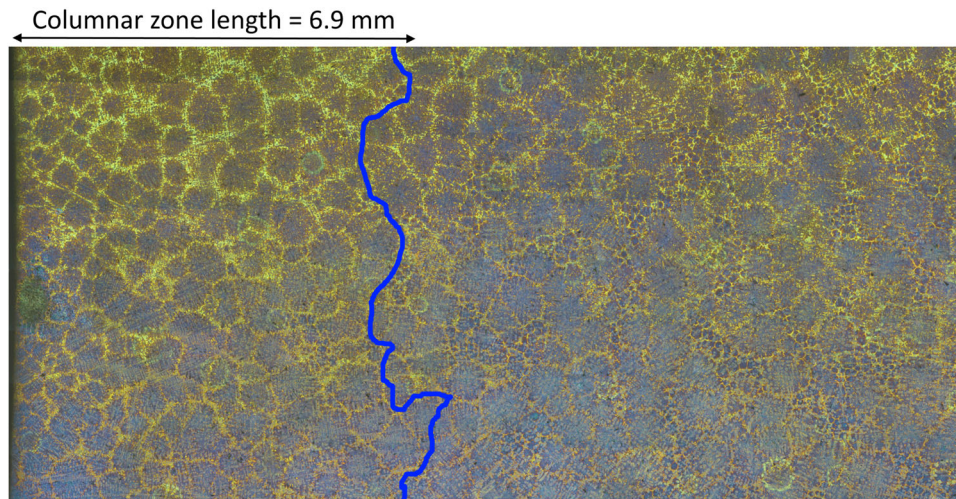
Columnar zone length = 6.9 mm

Figure 10. Color-etched microstructure of V3 in the region marked on Figure 3. Blue line marks columnar-to-equiaxed transition.

Table 2. Gradient Criterion of MagmaSoft® for Columnar, Transition and Equiaxed Regions of Volumes V1, V2, and V3

Volume	Gradient at columnar region (°C/mm)	Gradient at transition line (°C/mm)	Gradient at equiaxed region (°C/mm)
V1	3.3	1.1	0.8
V2	2.3	1.2	0.7
V3	2.1	1.2	0.4

Table 3. Number of Colonies per mm^2 for Volumes V1, V2, and V3

Volume	Colonies in columnar zone (mm^{-2})	Colonies in equiaxed zone (mm^{-2})
V1	5.0	3.3
V2	5.3	2.7
V3	4.0	2.0

Table 4. Cooling Rate Determined by MagmaSoft® for Columnar and Equiaxed Regions of Volumes V1, V2, and V3

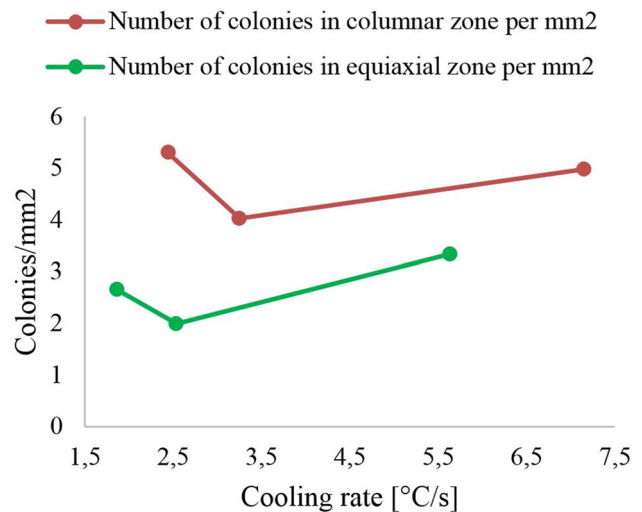| Volume	Cooling rate at columnar zone (°C/s)	Cooling rate at equiaxed zone (°C/s)
V1	7.2	5.6
V2	2.4	1.9
V3	3.3	2.5

Figure 11. Number of eutectic colonies per mm^2 in columnar and equiaxed zones as a function of cooling rate.

Table 5. Number of Austenite Grains per mm^2 for Volumes V1, V2, and V3

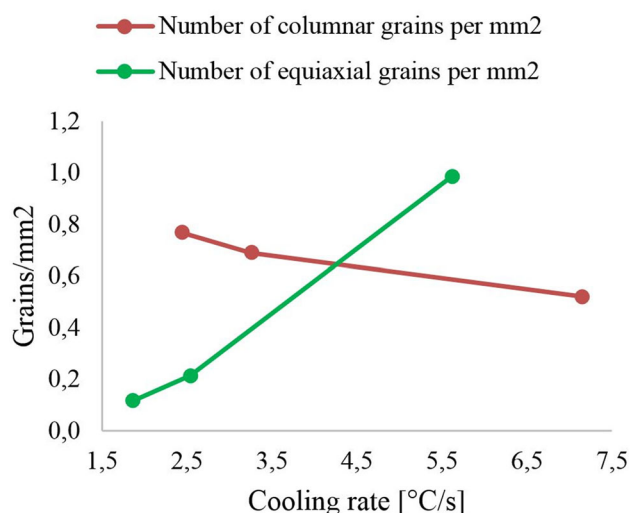| Vol.	Grains in columnar zone (mm^{-2})	Grains in equiaxed zone (mm^{-2})	Columnar/ equiaxed grains ratio
V1	0.5	1.0	0.53
V2	0.8	0.1	6.53
V3	0.7	0.2	3.24

Figure 12. Number of austenite grains per mm² in columnar and equiaxed zones as a function of cooling rate.

increase in cooling rate, the number of equiaxed grains increases, while the number of columnar grains remains nearly constant.

From the results of Table 5 and Figure 12, it arises that cooling rate is a key factor influencing the size of equiaxed grains, but not the size of columnar grains, at least within the current experimental conditions.

Conclusions

- The eutectic colonies or cells found in the microstructure have always the same crystalline orientation as the dendritic grain of austenite surrounding them, which means they are all part of the same austenite grain.
- A critical gradient value was found to define the columnar-to-equiaxed transition lines determined from the macrostructures by employing MagmaSoft®. Columnar zones have a value of gradient higher than the critical, while equiaxed regions have a lower value.
- For the samples studied, the size of the eutectic colonies at the columnar zone is smaller than the size of the eutectic colonies at the equiaxed zone.
- The size of equiaxed grains strongly decreases with the increase in cooling rate. On the other side, the size of the columnar grains remains almost invariable with the increase in cooling rate for the current experimental conditions.

REFERENCES

1. H. Morrogh, W. Oldfield, Iron Steel **32**, 431–434 (1959)
2. W. Oldfield, Br. Cast. Iron Res. Assoc. J. **9**, 177 (1960)
3. G. Ruff, J. Wallace, AFS Trans. **84**(705), 728 (1976)
4. H. Angus, *Cast Iron: Physical and Engineering Properties* (Butterworths, Oxford, 1976)
5. D. Stefanescu, *Metals Handbook, Casting* (ASM International, Cleveland, 1988)
6. M. Motz, Pract. Metallogr. **25**, 285–293 (1988)
7. G. Rivera, R. Boeri, J. Sikora, Cast Metals **8**, 1–5 (1995)
8. G. Rivera, R. Boeri, J. Sikora, Mater. Sci. Technol. **18**, 691–697 (2002)
9. G. Rivera, R. Boeri, J. Sikora, Scr. Mater. **50**, 331–335 (2004)
10. M. López, J. Massone, R. Boeri, Mater. Sci. Forum **925**, 110–117 (2018)
11. H. Fredriksson, U. Akerlind, *Solidification and Crystallization Processing in Metals and Alloys*, 1st edn. (Wiley, London, 2012)
12. E. Fras, M. Górny, Arch. Foundry Eng. **12**, 39–46 (2012)
13. N. Arab, Arch. Foundry Eng. **17**, 185–189 (2017)
14. D. Stefanescu, G. Alonso, P. Larrañaga, R. Suárez, Acta Mater. **103**, 103–114 (2016)
15. D. Stefanescu, A.S.M. Handbook, *Volume 1A: Cast Iron Science and Technology* (ASM International, Cleveland, 2017)
16. M. López, L. Brewer, J. Massone, R. Boeri, Metallogr. Microstruct. Anal. **8**, 1–7 (2019)
17. N. Tenaglia, R. Boeri, G. Rivera, J. Massone, Int. J. Cast Metals Res. **29**, 112–120 (2016)
18. M. López, G. Rivera, J. Massone, R. Boeri, Int. J. Cast Metals Res. **29**, 26–271 (2016)
19. MagmaSoft® v.5.2.0.10 Help Guide